

Intelligent Reflecting Surface-Assisted Multiple Access with User Pairing: NOMA or OMA?

Beixiong Zheng, *Member, IEEE*, Qingqing Wu, *Member, IEEE*, and Rui Zhang, *Fellow, IEEE*

Abstract—The integration of intelligent reflecting surface (IRS) to multiple access networks is a cost-effective solution for boosting spectrum/energy efficiency and enlarging network coverage/connections. However, due to the new capability of IRS in reconfiguring the wireless propagation channels, it is fundamentally unknown which multiple access scheme is superior in the IRS-assisted wireless network. In this letter, we pursue a theoretical performance comparison between non-orthogonal multiple access (NOMA) and orthogonal multiple access (OMA) in the IRS-assisted downlink communication, for which the transmit power minimization problems are formulated under the *discrete unit-modulus* reflection constraint on each IRS element. We analyze the minimum transmit powers required by different multiple access schemes and compare them numerically, which turn out to not fully comply with the *stereotyped superiority* of NOMA over OMA in conventional systems without IRS. Moreover, to avoid the exponential complexity of the brute-force search for the optimal discrete IRS phase shifts, we propose a low-complexity solution to achieve near-optimal performance.

Index Terms—Intelligent reflecting surface (IRS), non-orthogonal multiple access (NOMA), frequency division multiple access (FDMA), time division multiple access (TDMA), user pairing, power minimization, discrete phase shifts.

I. INTRODUCTION

INTELLIGENT reflecting surface (IRS) has recently attracted growing attention and is envisioned as an innovative technology for the beyond fifth-generation (B5G) communication system, due to its potential of achieving significant improvement in communication coverage, throughput, and energy efficiency [1]–[3]. Specifically, IRS is a planar metasurface composed of a large number of reconfigurable passive elements, which are attached with a smart controller to enable dynamic adjustment on the signal reflections for different purposes, such as signal power enhancement and interference suppression. In particular, compared to conventional techniques such as active relaying/beamforming, IRS not only reflects signals in a full-duplex and noise-free manner without incurring self-interference, but also greatly saves energy consumption and hardware/deployment cost by using lightweight passive components only [1], [3].

On the other hand, non-orthogonal multiple access (NOMA) has also received significant attention and shown superiority over orthogonal multiple access (OMA) in conventional wireless systems without IRS, for improving the spectral efficiency, balancing user fairness, and enlarging network connections. In the downlink NOMA, the user of stronger channel with the base station (BS) or access point (AP) employs the successive interference cancellation (SIC) technique to cancel the co-channel interference from the users of weaker channels, prior to decoding its own message. As a result, the decoding order depends on user channel power gains, which are determined by

The authors are with the Department of Electrical and Computer Engineering, National University of Singapore, email: {elezbe, elewqq, elezhang}@nus.edu.sg.

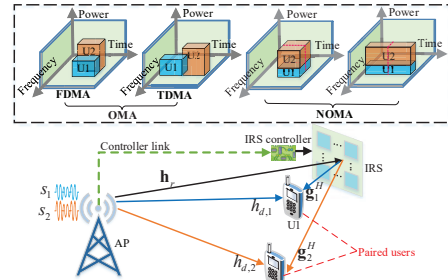


Fig. 1. An illustration of OMA and NOMA in the IRS-assisted system.

the propagation environments and user locations. In contrast, since IRS is capable of reconfiguring user channels by controlling the reflected signal amplitudes and/or phase shifts, the user decoding order of NOMA can be *permuted* by adjusting the IRS reflection to achieve more flexible performance trade-offs among the users. Nevertheless, for IRS to be integrated into the future wireless network, it still remains unknown whether NOMA is always superior to OMA as in conventional systems without IRS. Although some relevant works on the application of IRS to NOMA have recently appeared [4]–[7], the theoretical performance comparison between NOMA and OMA for IRS-assisted wireless communications is not well understood yet, to the best of our knowledge.

To address the above issue, in this letter we investigate the theoretical performance comparison between NOMA and OMA in an IRS-assisted downlink communication system, where two types of OMA schemes, i.e., frequency division multiple access (FDMA) and time division multiple access (TDMA), are considered, as shown in Fig. 1. The problems for minimizing the transmit power at the AP are formulated for both OMA and NOMA, subject to the *discrete unit-modulus reflection* constraint at the IRS and the users' target rates. By analyzing the relationship of minimum transmit powers required by different multiple access schemes, we unveil that the minimum transmit power of FDMA is always no lower than that of the other two counterparts (TDMA and NOMA), while the minimum power comparison between NOMA and TDMA depends on the target rates and locations of the users. Specifically, TDMA requires lower transmit power than NOMA when two near-IRS users are paired and have symmetric rates, whereas the relationship is reversed otherwise. Moreover, to avoid the exponentially high complexity of the brute-force search for the optimal discrete IRS phase shifts, we propose an efficient low-complexity algorithm based on the linear approximation initialization to effectively balance the user channel power gains for minimizing the transmit power, followed by the alternating optimization to achieve near-optimal performance.

II. SYSTEM MODEL AND PROBLEM FORMULATION

As depicted in Fig. 1, we consider an IRS-assisted downlink communication system, where an IRS is deployed to assist in

the transmission from a single-antenna AP to multiple single-antenna users. Similar to [8], [9], an IRS composed of N reflecting elements is divided into M sub-surfaces, each of which consists of $\bar{N} = N/M$ adjacent elements to share a common reflection coefficient for reducing the implementation complexity. Moreover, the passive IRS is connected to a smart controller that enables dynamic adjustment on the reflections of IRS elements and also plays the role of exchanging information between the IRS and AP via a separate wireless link [1], [3]. For ease of exposition, we focus on the case with any two users sharing two given adjacent time-frequency resource blocks (RBs) in practice, where the channels are assumed to be frequency-flat fading and constant over the two adjacent time-frequency RBs (see Fig. 1). It is worth pointing out that by adopting the concept of user pairing, the two-user case can be extended to the general multi-user case. Without loss of generality, it is assumed that user 1 is located in the vicinity of the IRS while user 2 can be arbitrarily located within the coverage of the AP (i.e., in or out of the IRS's coverage). As shown in Fig. 1, we consider two types of OMA schemes, i.e., FDMA and TDMA, which serve two users over two adjacent RBs separated in the frequency and time domains, respectively; while the NOMA scheme serves two users simultaneously over the two adjacent RBs either in the frequency- or time-domain, for fair comparison with OMA.

To characterize the optimal performance of different multiple access schemes in the IRS-assisted system, we assume perfect channel state information (CSI) available at the AP. Note that the channel estimation methods proposed in [1], [8] can be applied to acquire the CSI of the two users independently. The baseband equivalent channels from the AP to IRS, from the IRS to user k , and from the AP to user k are denoted by $\mathbf{h}_r \in \mathbb{C}^{M \times 1}$, $\mathbf{g}_k^H \in \mathbb{C}^{1 \times M}$, and $h_{d,k} \in \mathbb{C}$, respectively, with $k \in \{1, 2\}$. Let $\boldsymbol{\theta} \triangleq [\theta_1, \theta_2, \dots, \theta_M]^T = [\beta_1 e^{j\phi_1}, \beta_2 e^{j\phi_2}, \dots, \beta_M e^{j\phi_M}]^T$ denote the equivalent reflection coefficients of the IRS, where $\phi_m \in [0, 2\pi)$ and $\beta_m \in [0, 1]$ are the phase shift and reflection amplitude of the m -th sub-surface, respectively. To maximize the signal power reflected by the IRS and reduce the hardware cost, we set $\beta_m = 1, \forall m = 1, \dots, M$ and consider the practical discrete unit-modulus constraint $\mathcal{F} = \{e^{j\phi} | \phi \in \{0, \Delta\phi, \dots, (L-1)\Delta\phi\}\}$ for each phase shift coefficient θ_m , where $\Delta\phi = 2\pi/L$ with L denoting the number of discrete phase-shift levels [10].

A. NOMA Transmission Scheme

As shown in Fig. 1, the AP *simultaneously* transmits the signals of two users by adopting the superposition coding over two frequency/time domain adjacent RBs, which is given by

$$x = \sqrt{P_1} s_1 + \sqrt{P_2} s_2 \quad (1)$$

where P_k denotes the power allocated to user k with $k \in \{1, 2\}$ and s_k denotes the transmitted data symbol for user k , which is assumed to be a circularly symmetric complex Gaussian (CSCG) random variable with zero mean and unit variance. Accordingly, the signal received at user k is given by

$$y_k = (\mathbf{g}_k^H \boldsymbol{\Theta} \mathbf{h}_r + h_{d,k}) (\sqrt{P_1} s_1 + \sqrt{P_2} s_2) + n_k, k \in \{1, 2\} \quad (2)$$

where n_k denotes the additive CSCG noise with zero mean and variance σ^2 at user k and $\boldsymbol{\Theta} = \text{diag}(\boldsymbol{\theta})$ represents the diagonal phase-shift matrix of the IRS. By denoting $\mathbf{q}_k^H \triangleq \mathbf{g}_k^H \text{diag}(\mathbf{h}_r)$ as the cascaded AP-IRS-user channel before the IRS phase-shift adjustment, (2) can be rewritten as

$$y_k = (\mathbf{q}_k^H \boldsymbol{\theta} + h_{d,k}) (\sqrt{P_1} s_1 + \sqrt{P_2} s_2) + n_k, k \in \{1, 2\}. \quad (3)$$

Let $\lambda_1(\boldsymbol{\theta}) = |\mathbf{q}_1^H \boldsymbol{\theta} + h_{d,1}|^2$ and $\lambda_2(\boldsymbol{\theta}) = |\mathbf{q}_2^H \boldsymbol{\theta} + h_{d,2}|^2$ denote the channel power gains of users 1 and 2, respectively. Note that since channel power gains $\lambda_1(\boldsymbol{\theta})$ and $\lambda_2(\boldsymbol{\theta})$ are two discrete functions which vary with the IRS phase-shift vector $\boldsymbol{\theta}$, we may have $2! = 2$ permutations for the user decoding order. Given the target rates of the two users, we aim to minimize the total transmit power at the AP by optimizing the IRS phase-shift vector $\boldsymbol{\theta}$, subject to the discrete unit-modulus constraints of IRS elements. The corresponding optimization problem can be decomposed into two sub-problems associated with two different decoding orders as follows.

$$(N1): P_{N1} \triangleq \min_{\boldsymbol{\theta}, P_1, P_2} P_1 + P_2 \quad (4)$$

$$\text{s.t.} \quad \log_2 \left(1 + \frac{P_1 \lambda_1(\boldsymbol{\theta})}{\sigma^2} \right) \geq \gamma_1 \quad (5)$$

$$\log_2 \left(1 + \frac{P_2 \lambda_2(\boldsymbol{\theta})}{\sigma^2 + P_1 \lambda_2(\boldsymbol{\theta})} \right) \geq \gamma_2 \quad (6)$$

$$\theta_m \in \mathcal{F}, \forall m = 1, \dots, M \quad (7)$$

$$(N2): P_{N2} \triangleq \min_{\boldsymbol{\theta}, P_1, P_2} P_1 + P_2 \quad (8)$$

$$\text{s.t.} \quad \log_2 \left(1 + \frac{P_1 \lambda_1(\boldsymbol{\theta})}{\sigma^2 + P_2 \lambda_1(\boldsymbol{\theta})} \right) \geq \gamma_1 \quad (9)$$

$$\log_2 \left(1 + \frac{P_2 \lambda_2(\boldsymbol{\theta})}{\sigma^2} \right) \geq \gamma_2 \quad (10)$$

$$\theta_m \in \mathcal{F}, \forall m = 1, \dots, M \quad (11)$$

where γ_1 and γ_2 are the target rates of users 1 and 2 in bits per second per Hertz (bps/Hz), respectively. Since the user rates are monotonically increasing with P_1 and P_2 , the inequality rate constraints should be met with equality at the optimal solution. By eliminating the equality constraints, (N1) and (N2) can be simplified as

$$(N1.1): P_{N1} \triangleq \min_{\boldsymbol{\theta}} \frac{(2^{\gamma_1} - 1) 2^{\gamma_2} \sigma^2}{\lambda_1(\boldsymbol{\theta})} + \frac{(2^{\gamma_2} - 1) \sigma^2}{\lambda_2(\boldsymbol{\theta})} \quad (12)$$

$$\text{s.t.} \quad \theta_m \in \mathcal{F}, \forall m = 1, \dots, M \quad (13)$$

$$(N2.1): P_{N2} \triangleq \min_{\boldsymbol{\theta}} \frac{(2^{\gamma_1} - 1) \sigma^2}{\lambda_1(\boldsymbol{\theta})} + \frac{(2^{\gamma_2} - 1) 2^{\gamma_1} \sigma^2}{\lambda_2(\boldsymbol{\theta})} \quad (14)$$

$$\text{s.t.} \quad \theta_m \in \mathcal{F}, \forall m = 1, \dots, M. \quad (15)$$

Comparing (12) and (14), we have

$$\begin{aligned} & \frac{(2^{\gamma_1} - 1) 2^{\gamma_2} \sigma^2}{\lambda_1(\boldsymbol{\theta})} + \frac{(2^{\gamma_2} - 1) \sigma^2}{\lambda_2(\boldsymbol{\theta})} - \frac{(2^{\gamma_1} - 1) \sigma^2}{\lambda_1(\boldsymbol{\theta})} - \frac{(2^{\gamma_2} - 1) 2^{\gamma_1} \sigma^2}{\lambda_2(\boldsymbol{\theta})} \\ &= (2^{\gamma_1} - 1)(2^{\gamma_2} - 1) \sigma^2 \left(\frac{1}{\lambda_1(\boldsymbol{\theta})} - \frac{1}{\lambda_2(\boldsymbol{\theta})} \right) \end{aligned} \quad (16)$$

which is non-positive for $\lambda_1(\boldsymbol{\theta}) \geq \lambda_2(\boldsymbol{\theta})$ and non-negative for $\lambda_2(\boldsymbol{\theta}) \geq \lambda_1(\boldsymbol{\theta})$, respectively. Thus, the minimum power required by using NOMA is obtained as

$$P_N \triangleq \min\{P_{N1}, P_{N2}\} = \begin{cases} P_{N1}, & \lambda_1(\boldsymbol{\theta}_N^*) \geq \lambda_2(\boldsymbol{\theta}_N^*) \\ P_{N2}, & \text{otherwise} \end{cases} \quad (17)$$

with $\boldsymbol{\theta}_N^*$ being the optimal phase-shift vector.

B. OMA Transmission Schemes

1) *FDMA*: As shown in Fig. 1, the AP communicates with two users *simultaneously* over two equal frequency-domain adjacent RBs via FDMA. Accordingly, the optimization problem of minimizing the total transmit power at the AP is formulated as

$$(F1): P_F \triangleq \min_{\boldsymbol{\theta}, P_1, P_2} P_1 + P_2 \quad (18)$$

$$\text{s.t.} \quad \frac{1}{2} \log_2 \left(1 + \frac{P_1 \lambda_1(\boldsymbol{\theta})}{\frac{1}{2} \sigma^2} \right) \geq \gamma_1 \quad (19)$$

$$\frac{1}{2} \log_2 \left(1 + \frac{P_2 \lambda_2(\boldsymbol{\theta})}{\frac{1}{2} \sigma^2} \right) \geq \gamma_2 \quad (20)$$

$$\theta_m \in \mathcal{F}, \forall m = 1, \dots, M. \quad (21)$$

Note that the factor 1/2 in (19) and (20) is due to the fact that each user is assigned with half of the bandwidth as compared to the case of NOMA. Similar to NOMA, the inequality rate constraints can be replaced with equality constraints and problem (F1) is transformed into

$$(F1.1): P_F \triangleq \min_{\boldsymbol{\theta}} \frac{(2^{2\gamma_1} - 1)\sigma^2}{2\lambda_1(\boldsymbol{\theta})} + \frac{(2^{2\gamma_2} - 1)\sigma^2}{2\lambda_2(\boldsymbol{\theta})} \quad (22)$$

$$\text{s.t.} \quad \theta_m \in \mathcal{F}, \forall m = 1, \dots, M. \quad (23)$$

2) *TDMA*: As shown in Fig. 1, the AP communicates with two users *consecutively* over two equal time-domain adjacent RBs via TDMA. Different from NOMA and FDMA where the IRS phase-shift vector needs to be set identical for the two users, in the case of TDMA the IRS phase-shift vector can be set different for the two users over different time. This is fundamentally due to the hardware limitation of IRS passive reflection, which can be made *time-selective*, but not *frequency-selective* [1]. Thus, the optimization problem of minimizing the total transmit power at the AP in the case of TDMA can be formulated as

$$(T1): P_T \triangleq \min_{\boldsymbol{\theta}_1, \boldsymbol{\theta}_2, P_1, P_2} P_1 + P_2 \quad (24)$$

$$\text{s.t.} \quad \frac{1}{2} \log_2 \left(1 + \frac{2P_1 \lambda_1(\boldsymbol{\theta}_1)}{\sigma^2} \right) \geq \gamma_1 \quad (25)$$

$$\frac{1}{2} \log_2 \left(1 + \frac{2P_2 \lambda_2(\boldsymbol{\theta}_2)}{\sigma^2} \right) \geq \gamma_2 \quad (26)$$

$$\theta_{k,m} \in \mathcal{F}, \forall m = 1, \dots, M, k \in \{1, 2\} \quad (27)$$

where $\boldsymbol{\theta}_k \triangleq [\theta_{k,1}, \theta_{k,2}, \dots, \theta_{k,M}]^T$ denotes the phase-shift vector for the k -th user. Note that the factor 1/2 in (25) and (26) is due to the fact that each user is assigned with half of the time as compared to the case of NOMA; as a result, there is an equivalent power gain of 2 for each user shown in (25) and (26) for fair comparison with NOMA. Similar to (F1), (T1) can be transformed into

$$(T1.1): P_T \triangleq \min_{\boldsymbol{\theta}_1} \frac{(2^{2\gamma_1} - 1)\sigma^2}{2\lambda_1(\boldsymbol{\theta}_1)} + \min_{\boldsymbol{\theta}_2} \frac{(2^{2\gamma_2} - 1)\sigma^2}{2\lambda_2(\boldsymbol{\theta}_2)} \quad (28)$$

$$\text{s.t.} \quad \theta_{k,m} \in \mathcal{F}, \forall m = 1, \dots, M, k \in \{1, 2\}. \quad (29)$$

III. PERFORMANCE COMPARISON AND LOW-COMPLEXITY SOLUTION

A. Comparison of Minimum Transmit Power

First, we compare the minimum transmit powers required by FDMA and TDMA for the IRS-assisted system, whose relationship is given by the following proposition.

Proposition 1: As the minimum of the sum of two functions is no less than the sum of their individual minimum values, it follows that $P_F \geq P_T$ by comparing (22) and (28), and the equality holds if and only if

$$\arg \max_{\boldsymbol{\theta} \in \mathcal{F}^M} \lambda_1(\boldsymbol{\theta}) = \arg \max_{\boldsymbol{\theta} \in \mathcal{F}^M} \lambda_2(\boldsymbol{\theta}). \quad (30)$$

Note that the above result is a direct consequence of passive IRS reflection that can be *time-selective*, but cannot be *frequency-selective*.

Next, we compare the minimum transmit powers required by FDMA and NOMA for the IRS-assisted system, with the result given by the following proposition.

Proposition 2: The minimum transmit powers required by NOMA and FDMA satisfy $P_F \geq P_N$, and the equality holds if and only if $\boldsymbol{\theta}_N^* = \boldsymbol{\theta}_F^*$, $\lambda_1(\boldsymbol{\theta}_F^*) = \lambda_2(\boldsymbol{\theta}_F^*)$, and $\gamma_1 = \gamma_2$.

Proof: Let $\boldsymbol{\theta}_F^*$ denote the optimal phase-shift vector for (F1.1) associated with FDMA. For the case of $\lambda_1(\boldsymbol{\theta}_F^*) \geq \lambda_2(\boldsymbol{\theta}_F^*)$, the power gap between (12) and (22) is given by

$$\begin{aligned} \Delta P_1 &= P_F - P_{N1} \\ &\stackrel{(a)}{\geq} \frac{(2^{2\gamma_1} - 1)\sigma^2}{2\lambda_1(\boldsymbol{\theta}_F^*)} + \frac{(2^{2\gamma_2} - 1)\sigma^2}{2\lambda_2(\boldsymbol{\theta}_F^*)} - \frac{(2^{\gamma_1} - 1)2^{\gamma_2}\sigma^2}{\lambda_1(\boldsymbol{\theta}_F^*)} - \frac{(2^{\gamma_2} - 1)\sigma^2}{\lambda_2(\boldsymbol{\theta}_F^*)} \\ &= \frac{(2^{2\gamma_1} - 1 - 2^{\gamma_1 + \gamma_2 + 1} + 2^{\gamma_2 + 1})\sigma^2}{2\lambda_1(\boldsymbol{\theta}_F^*)} + \frac{(2^{2\gamma_2} - 2^{\gamma_2 + 1} + 1)\sigma^2}{2\lambda_2(\boldsymbol{\theta}_F^*)} \\ &\stackrel{(b)}{\geq} \frac{(2^{2\gamma_2} - 2^{\gamma_1 + \gamma_2 + 1} + 2^{2\gamma_1})\sigma^2}{2\lambda_1(\boldsymbol{\theta}_F^*)} \\ &= \frac{(2^{\gamma_2} - 2^{\gamma_1})^2 \sigma^2}{2\lambda_1(\boldsymbol{\theta}_F^*)} \stackrel{(c)}{\geq} 0 \end{aligned} \quad (31)$$

where the equality of (a) holds if $\boldsymbol{\theta}_F^*$ is also an optimal solution to problem (N1.1); the equality of (b) holds when $\lambda_1(\boldsymbol{\theta}_F^*) = \lambda_2(\boldsymbol{\theta}_F^*)$; and the equality of (c) holds when $\gamma_1 = \gamma_2$. Similarly, for the case of $\lambda_2(\boldsymbol{\theta}_F^*) \geq \lambda_1(\boldsymbol{\theta}_F^*)$, we can also obtain a non-negative power gap between (14) and (22), i.e., $\Delta P_2 = P_F - P_{N2} \geq 0$. Since $P_F \geq P_{N1}$ and $P_F \geq P_{N2}$, we can conclude that $P_F \geq \min\{P_{N1}, P_{N2}\} = P_N$, where the equality holds when the above conditions are all satisfied. ■

Remark 1: From the above two propositions, we obtain $P_F \geq P_T$ and $P_F \geq P_N$, which implies that the minimum transmit power required by FDMA is always no lower than that of TDMA or NOMA. However, there is no deterministic relationship between the minimum transmit power with NOMA versus that with TDMA, which generally depends on the locations and target rates of the two users, as will be shown later in Section IV by numerical examples.

B. Optimal Solution

Due to the discrete unit-modulus constraint on $\boldsymbol{\theta}$ and the non-convex objective functions, there is no standard method

for efficiently solving the non-convex optimization problems (N1.1), (N2.1), (F1.1), and (T1.1) with globally optimal solutions. One straightforward approach is to search for all possible combinations of discrete phase shifts at all sub-surfaces and choose the one that achieves the minimum transmit power. However, such a brute-force search method incurs an exponential complexity of $\mathcal{O}(L^M)$, which is prohibitively high for practical systems with large M and/or L . Although other approaches such as the branch-and-bound method can be applied to reduce the complexity [10], the worst-case complexity is still exponential over M due to the fundamental NP-hardness. Thus, it mainly serves as a benchmark for evaluating other suboptimal schemes.

C. Suboptimal Solution

Note that the objective functions of (12), (14) for NOMA, and (22) for FDMA are the weighed sum of two inverse channel power gains, which can be expressed in a generic form as

$$Q(\boldsymbol{\theta}) = \frac{a_1}{\lambda_1(\boldsymbol{\theta})} + \frac{a_2}{\lambda_2(\boldsymbol{\theta})}, \quad \theta_m \in \mathcal{F}, \forall m = 1, \dots, M \quad (32)$$

where a_1 and a_2 are two positive constants. Dropping the discrete constraint, the phase-shift vector that maximizes only each of the two user channel power gains is given by

$$\mathbf{u}_k = \arg \max_{\boldsymbol{\psi}} \lambda_k(\boldsymbol{\psi}) = e^{j\angle h_{a,k}} e^{j\angle \mathbf{q}_k}, \quad k \in \{1, 2\} \quad (33)$$

where $\angle(\cdot)$ returns the phase of each element and $\boldsymbol{\psi} \triangleq [\psi_1, \psi_2, \dots, \psi_M]^T$ with $|\psi_m| = 1, \forall m = 1, \dots, M$. Note that $\mathbf{u}_1 \neq \mathbf{u}_2$ in general, which implies that one phase-shift vector $\boldsymbol{\psi}$ cannot maximize two channel power gains $\lambda_1(\boldsymbol{\psi})$ and $\lambda_2(\boldsymbol{\psi})$ at the same time. As such, $\boldsymbol{\psi}$ needs to be properly designed to balance the channel power gains of two users for minimizing $Q(\boldsymbol{\psi})$ in (32).

To this end, we first define the non-negative linear combination of \mathbf{u}_1 and \mathbf{u}_2 as

$$\bar{\mathbf{u}}^{[\eta]} \triangleq \eta \mathbf{u}_1 + (1 - \eta) \mathbf{u}_2, \quad 0 \leq \eta \leq 1. \quad (34)$$

As $\bar{\mathbf{u}}^{[\eta]}$ may not satisfy the unit-modulus constraint, we try to find its nearest unit-modulus vector $\tilde{\mathbf{u}}^{[\eta]}$, which is given by

$$\tilde{\mathbf{u}}^{[\eta]} = \arg \min_{\boldsymbol{\psi}} \left\| \boldsymbol{\psi} - \bar{\mathbf{u}}^{[\eta]} \right\|^2 = e^{j\angle \bar{\mathbf{u}}^{[\eta]}}, \quad 0 \leq \eta \leq 1 \quad (35)$$

to achieve a good balance between the two channel power gains by varying η . For simplicity, we divide $[0, 1]$ into $B + 1$ equal levels, which are denoted by the set $\mathcal{B} = \{0, \frac{1}{B}, \dots, \frac{B-1}{B}, 1\}$. Then, for each $\eta \in \mathcal{B}$, we quantize each phase shift in $\tilde{\mathbf{u}}^{[\eta]}$ to its nearest point in \mathcal{F} to obtain the discrete phase-shift vector $\boldsymbol{\theta}^{[\eta]}$, with each element given by

$$\theta_m^{[\eta]} = \arg \min_{\theta \in \mathcal{F}} \left| \theta - \tilde{u}_m^{[\eta]} \right|^2, \quad m = 1, \dots, M. \quad (36)$$

Finally, we obtain the suboptimal solution $\boldsymbol{\theta}^{[\eta^*]}$ according to

$$\eta^* = \arg \min_{\eta \in \mathcal{B}} \frac{a_1}{\lambda_1(\boldsymbol{\theta}^{[\eta]})} + \frac{a_2}{\lambda_2(\boldsymbol{\theta}^{[\eta]})}. \quad (37)$$

From the above, we see that (N1.1), (N2.1), and (F1.1) can be solved suboptimally based on (36) and (37) with a linear complexity of $\mathcal{O}(BML)$ only, which is thus referred



Fig. 2. Two deployment cases of the AP, IRS, and two users (top view), where $d_A = 50$ m and $d_I = 4$ m.

to as the linear approximation (LA) method. Furthermore, to further improve the solution obtained in (36) and (37), the alternating optimization (AO) method [10] can be applied to solve (32) based on the initial solution obtained by the LA method. Specifically, we alternately optimize one phase shift θ_m via one-dimensional search over \mathcal{F} while fixing the other $M - 1$ phase shifts $\{\theta_i\}_{i \neq m}$, and iterate the above until the convergence is reached. Note that the proposed algorithm is guaranteed to converge since the objective value of (32) is non-increasing over the iterations and lower-bounded by a finite value $\frac{a_1}{\lambda_1(\mathbf{u}_1)} + \frac{a_2}{\lambda_2(\mathbf{u}_2)}$. Given the number of iterations I , the total complexity of the proposed algorithm is $\mathcal{O}((B+I)ML)$.

On the other hand, for (T1.1) associated with TDMA, since θ_1 and θ_2 are decoupled in the objective function of (28), we can simply quantize each phase shift in \mathbf{u}_1 and \mathbf{u}_2 to its nearest point in \mathcal{F} to obtain discrete phase-shift vectors $\boldsymbol{\theta}_1^*$ and $\boldsymbol{\theta}_2^*$, with each element given by

$$\theta_{k,m}^* = \arg \min_{\theta \in \mathcal{F}} |\theta - u_{k,m}|^2, \quad m=1, \dots, M, k \in \{1, 2\}. \quad (38)$$

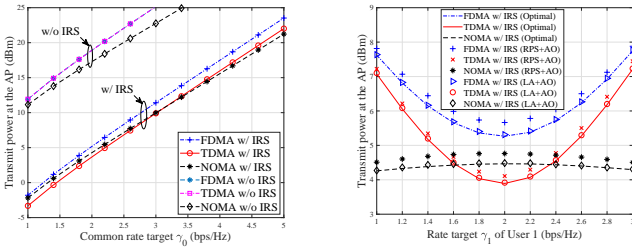
With the above for initialization, the AO method can be similarly applied to refine the solution to (T1.1). The overall complexity is thus of $\mathcal{O}((2+I)ML)$.

IV. SIMULATION RESULTS

In this section, we present simulation results to numerically validate our analytical results (Propositions 1 and 2) and compare the performance of OMA (TDMA and FDMA) with NOMA in an IRS-assisted two-user system. The total number of reflecting elements of the IRS is set to $N = 100$, which is divided into $M = 5$ sub-surfaces.¹ The path loss exponents of the AP→users, IRS→users, and AP→IRS links are set as 3.2, 2.6, and 2.5, respectively, and the path loss at the reference distance of 1 meter (m) is set as 30 dB for each individual link [3], [8], [10]. Moreover, the small-scale fading is characterized by Rayleigh fading for each individual link. We consider two deployment cases shown in Fig. 2, where $d_I = 4$ m and $d_A = 50$ m. The results are averaged over 100 independent fading channel realizations, with $L = 8$ and $\sigma^2 = -80$ dBm.

We first consider Case 1 in Fig. 2, where the two users are both located in the vicinity of the IRS with equal distances from the IRS as well as the AP. In Fig. 3(a), we compare the AP transmit powers required by different multiple access schemes versus the common target rate $\gamma_1 = \gamma_2 = \gamma_0$ for the two users. Apparently, compared to the schemes without IRS, the required transmit power at the AP is significantly reduced with the aid of IRS. Moreover, one can observe that without IRS, the required transmit power by NOMA is always lower than that of OMA (same for TDMA and FDMA). In contrast,

¹The number of sub-surfaces is kept to be small for implementing the brute-force search to obtain the optimal solution and provide the performance upper bound for the proposed algorithm.



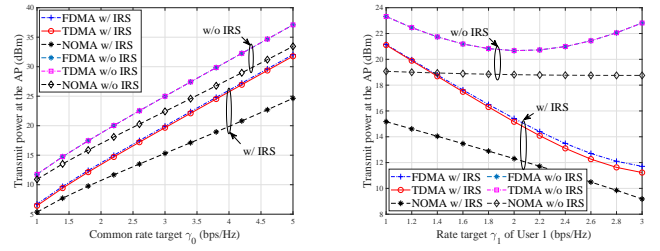
(a) AP transmit power versus the common target rate γ_0 . (b) AP transmit power versus user 1's target rate γ_1 , with the two users' sum rate fixed as $\gamma_1 + \gamma_2 = 4$ bps/Hz.

Fig. 3. Performance comparison of OMA and NOMA in Case 1.

when the IRS is deployed to assist two users in its vicinity, the above conclusion is not valid in general. For example, we observe that the required transmit power by TDMA is lower than that of NOMA for the common target rate γ_0 less than 3 bps/Hz. This is due to the use of different IRS phase-shift designs for the two users by exploiting the IRS's time selectivity via TDMA. Moreover, FDMA always requires higher transmit power than the other two counterparts, which is in accordance with Propositions 1 and 2. On the other hand, by increasing the common target rate γ_0 , the power growth rate with TDMA is slightly higher than that with NOMA, which can be well understood since the required power by TDMA in (28) is the sum of two exponential functions with a higher exponent of $2\gamma_0$, as compared to that in (12) or (14) with NOMA.

To draw more insight for Case 1, we depict the AP transmit powers required by different transmission schemes versus user 1's target rate γ_1 in Fig. 3(b), with the two users' sum rate fixed as $\gamma_1 + \gamma_2 = 4$ bps/Hz. First, we can observe that TDMA requires lower transmit power than NOMA when the target rates of the two users are close (i.e., symmetric). Second, the transmit powers of both TDMA and FDMA are observed to dramatically increase when the two users' rates become more *asymmetric*, which is attributed to the exponentially increasing of the dominant user target rate, i.e., $\max\{\gamma_1, \gamma_2\}$ in (22) and (28). In contrast, it is observed that the required transmit power by NOMA is almost insensitive to the disparity of user target rates, thus providing a more robust performance. Third, to show the performance of the proposed suboptimal solution in Section III-C (i.e., the LA method with $B = 8$ followed by the AO method with $I = 2$), we consider two benchmark schemes: 1) the optimal solution by the brute-force search and 2) the random phase shift (RPS) initialization followed by the AO method with 10 iterations (which has the same complexity as the proposed one for fair comparison). One can observe that our proposed solution achieves near-optimal performance, whereas a non-negligible performance loss is observed for the RPS-based initialization as compared to the optimal solution. The above result shows the effectiveness of the low-complexity LA method.

Next, unlike Case 1 with two near-IRS users (namely, *symmetric* user deployment), we consider another setup of Case 2 with one near-IRS user and one far-IRS user (namely, *asymmetric* user deployment). As one user moves far away from the IRS and thus needs more power directly from the AP, it is observed in Figs. 4(a) and 4(b) that the transmit



(a) AP transmit power versus the common target rate γ_0 . (b) AP transmit power versus user 1's target rate γ_1 , with the two users' sum rate fixed as $\gamma_1 + \gamma_2 = 4$ bps/Hz.

Fig. 4. Performance comparison of OMA and NOMA in Case 2.

power required at the AP increases drastically compared to Figs. 3(a) and 3(b). This is expected since it is more energy efficient when both users are located in the vicinity of the IRS to reap its passive beamforming gain for saving the AP transmit power. Moreover, one can observe from Figs. 4(a) and 4(b) that the required transmit power by NOMA is always lower than that by OMA, regardless of whether TDMA or FDMA is used. This can be explained by the fact that NOMA has higher spectrum efficiency than OMA under *asymmetric* user channels, even with IRS deployed to assist one of the two users. Furthermore, since the IRS reflection has negligible effect on the far-IRS user, TDMA and FDMA show nearly the same performance in the IRS-assisted system.

V. CONCLUSIONS

In this letter, we have optimized the IRS reflection with *discrete phase shifts* for the IRS-assisted NOMA and OMA systems to minimize the AP transmit power with given user rates. The minimum transmit powers required by different multiple access schemes have been compared analytically and a low-complexity algorithm has been proposed to achieve near-optimal performance. In particular, our work has revealed that NOMA may perform worse than TDMA for near-IRS users with *symmetric* rates. This thus provides an important guideline for user pairing in IRS-aided systems with a large number of users and RBs (e.g., IRS-assisted orthogonal FDMA (OFDMA)): it is preferable to pair users with *asymmetric* rates and/or *asymmetric* deployment (i.e., with distinct distances from the IRS, regardless of the distances from the AP) to exploit the NOMA gain over OMA.

REFERENCES

- [1] Q. Wu and R. Zhang, "Towards smart and reconfigurable environment: Intelligent reflecting surface aided wireless network," *IEEE Commun. Mag.*, doi: 10.1109/MCOM.001.1900107, Nov. 2019.
- [2] M. Di Renzo *et al.*, "Smart radio environments empowered by reconfigurable AI meta-surfaces: An idea whose time has come," *EURASIP J. Wireless Commun. Netw.*, vol. 2019:129, May 2019.
- [3] Q. Wu and R. Zhang, "Intelligent reflecting surface enhanced wireless network via joint active and passive beamforming," *IEEE Trans. Wireless Commun.*, vol. 18, no. 11, pp. 5394–5409, Nov. 2019.
- [4] G. Yang, X. Xu, and Y.-C. Liang, "Intelligent reflecting surface assisted non-orthogonal multiple access," *arXiv preprint arXiv:1907.03133*, 2019.
- [5] Z. Ding and H. Poor, "A simple design of IRS-NOMA transmission," *arXiv preprint arXiv:1907.09918*, 2019.
- [6] Y. Li, M. Jiang, Q. Zhang, and J. Qin, "Joint beamforming design in multi-cluster MISO NOMA intelligent reflecting surface-aided downlink communication networks," *arXiv preprint arXiv:1909.06972*, 2019.

- [7] X. Mu, Y. Liu, L. Guo, J. Lin, and N. Al-Dhahir, "Exploiting intelligent reflecting surfaces in multi-antenna aided NOMA systems," *arXiv preprint arXiv:1910.13636*, 2019.
- [8] B. Zheng and R. Zhang, "Intelligent reflecting surface-enhanced OFDM: Channel estimation and reflection optimization," *IEEE Wireless Commun. Lett.*, doi: 10.1109/LWC.2019.2961357, Dec. 2019.
- [9] Y. Yang, B. Zheng, S. Zhang, and R. Zhang, "Intelligent reflecting surface meets OFDM: Protocol design and rate maximization," *arXiv preprint arXiv:1906.09956*, 2019.
- [10] Q. Wu and R. Zhang, "Beamforming optimization for wireless network aided by intelligent reflecting surface with discrete phase shifts," *IEEE Trans. Commun.*, doi: 10.1109/TCOMM.2019.2958916, Dec. 2019.